

Structural disorder and magnetism in the spin-gapless semiconductor CoFeCrAl

Renu Choudhary,^{1,2} Parashu Kharel,³ Shah R. Valloppilly,² Yunlong Jin,²
Andrew O'Connell,² Yung Huh,³ Simeon Gilbert,³ Arti Kashyap,¹
D. J. Sellmyer,² and Ralph Skomski²

¹*School of Basic Sciences, Indian Institute of Technology, Mandi, Himachal Pradesh, India*

²*Department of Physics and Astronomy and NCMN, University of Nebraska, Lincoln, NE 68588, USA*

³*Department of Physics, South Dakota State University, Brookings, SD 57007, USA*

(Presented 14 January 2016; received 4 November 2015; accepted 16 December 2015;
published online 4 March 2016)

Disordered CoFeCrAl and CoFeCrSi_{0.5}Al_{0.5} alloys have been investigated experimentally and by first-principle calculations. The melt-spun and annealed samples all exhibit Heusler-type superlattice peaks, but the peak intensities indicate a substantial degree of B2-type chemical disorder. Si substitution reduces the degree of this disorder. Our theoretical analysis also considers several types of antisite disorder (Fe-Co, Fe-Cr, Co-Cr) in Y-ordered CoFeCrAl and partial substitution of Si for Al. The substitution transforms the spin-gapless semiconductor CoFeCrAl into a half-metallic ferrimagnet and increases the half-metallic band gap by 0.12 eV. Compared CoFeCrAl, the moment of CoFeCrSi_{0.5}Al_{0.5} is predicted to increase from 2.01 μ_B to 2.50 μ_B per formula unit, in good agreement with experiment. © 2016 Author(s). All article content, except where otherwise noted, is licensed under a Creative Commons Attribution 3.0 Unported License. [<http://dx.doi.org/10.1063/1.4943306>]

I. INTRODUCTION

Spin-gapless semiconductors (SGS) have recently attracted much attention as nanoelectronic materials with high carrier mobility and good semiconductor impedance match. Y-ordered CoFeCrAl is one of the few SGS for which both theoretical¹⁻³ and preliminary experimental results⁴⁻⁶ are available. SGS are characterized by a zero band gap for majority electrons and a finite band gap for minority electrons, so that disorder has a pronounced impact on electronic structure and transport. CoFeCrAl is a particularly intriguing case due to the potential of several closely related Heusler and non-Heusler phases.³

One challenge is to create an alloy crystallizing in a Heusler phase (L2₁ or Y), as contrasted to the B2 (CsCl) phase. The former require a superlattice ordering of the Cr and Al atoms, whereas in the latter, Cr and Al form a solid solution. Figure 1 shows the structures of the involved phases. A B2 phase has been obtained in Ref. 5, whereas the phase investigated in Ref. 4 is of the Heusler type. However, the corresponding (111) superlattice peak in Ref. 3 is relatively weak, which indicates substantial B2-type chemical order, and the question arises how the degree of L2₁ or Y order can be improved. Another consideration is substitutional chemical disorder. For example, the structural, electronic and magnetic properties of the Fe doped half-Heusler and Heusler compounds CoFe_xCrAl and Co_{2-x}Fe_xCrAl ($x = 0, 0.25, 0.5, 0.75, 1.0$), respectively, have been studied both experimentally⁷ and theoretically.⁸

In this paper, we use density-functional theory (DFT) and experiment to investigate chemical disorder in CoFeCrAl and the effect of the partial substitution of Si for Al. Chemical disorder tends to transform the spin-gapless semiconductor (SGS) into half-metallic magnets. However, Si addition improves the degree of Heusler ordering and changes the electronic structure from a SGS to a half-metal with increased minority band gap.



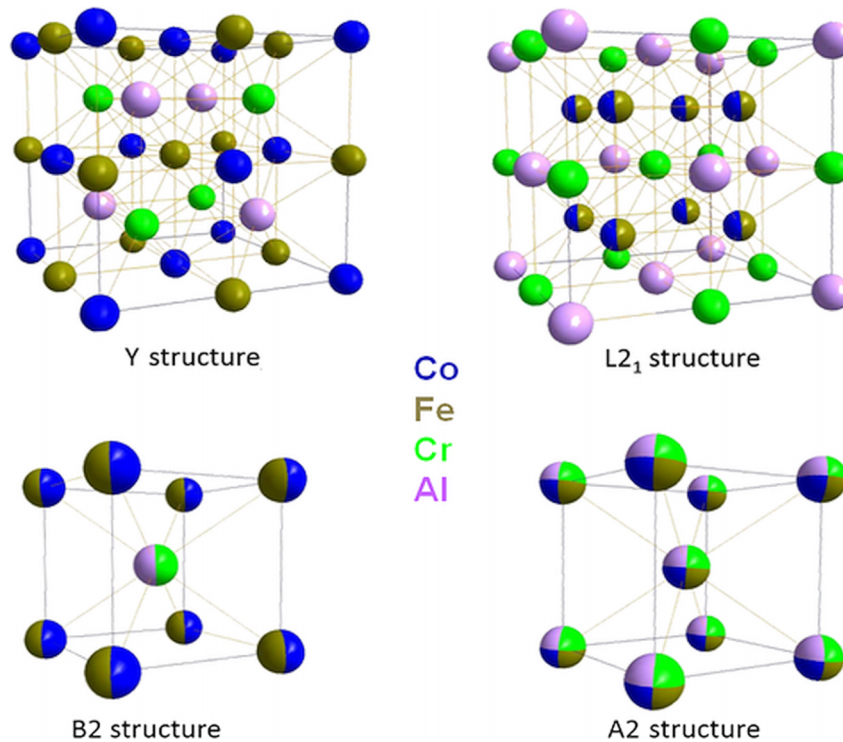


FIG. 1. Effect of chemical disorder in CoFeCrAl alloys. No disorder is allowed in the perfect Y-type CoFeCrAl structure (space group $F43m$), whereas Co-Fe solid-solubility yields the cubic Heusler or $L2_1$ structure. With further increasing degree of disorder, the CsCl or B2 structure distinguishes two types of occupancies (Fe-Co and Cr-Al) and the fcc (A2) structure is completely random with respect to atomic positions.

II. RESULTS AND DISCUSSION

A. Experimental Results

In order to investigate the effect of partial replacement of Al by Si on the structure and magnetism of CoFeCrAl, we have produced and analyzed two melt-spun CoFeCrAl_{0.5}Si_{0.5} ribbon samples. The two samples were produced by arc melting, rapid quenching, and annealing in vacuum (10^{-7} torr) for 4 h, one at 450 °C for 4 h and the other at 750 °C. The ribbons were ground into powder and placed on a low-background Si plate and spun continuously during Cu-radiation X-ray diffraction using a PANalytical Empyrean diffractometer. Full pattern structure refinement and quantification was performed using the Total Pattern Analysis Solutions Software (TOPAS). Magnetic properties were investigated using Quantum Design Physical Properties Measurement system (PPMS).

Figure 2(a) shows the x-ray diffraction pattern for the sample annealed at 450 °C as well as the fit and difference curves obtained from Rietveld analysis. The patterns are identical to that of CoFeCrAl, which are rather close to the disordered $L2_1$ Heusler structure.⁴ The sample annealed at 450 °C is nearly single-phase, but annealing at 750 °C yields cubic $Cr_3(Al, Si)$ and $Co(Fe, Al)$ impurities. Estimated from Rietveld analysis, the amounts of the impurity phases are 21 wt.% (750 °C) and 7 wt.% (450 °C).

The Si substitution for Al enhances the intensity of the superlattice reflections (111) and (200) as compared to CoFeCrAl. In CoFeCrAl, about 35% of the Cr and Al exchange their positions.⁴ In CoFeCrAl_{0.5}Si_{0.5} annealed at 450 °C, the site ordering between Cr and (Al, Si) increases to about 28% exchanged atoms. In other words, Si substitution reduces the B2-type disorder and promotes Heusler-type ordering. Note that $L2_1$ and Y structures are virtually impossible to distinguish by XRD, but the magnetic exchange interaction could be significantly influenced due to reordering at higher temperature. The lattice parameter a decreases upon Si substitution, as expected from the

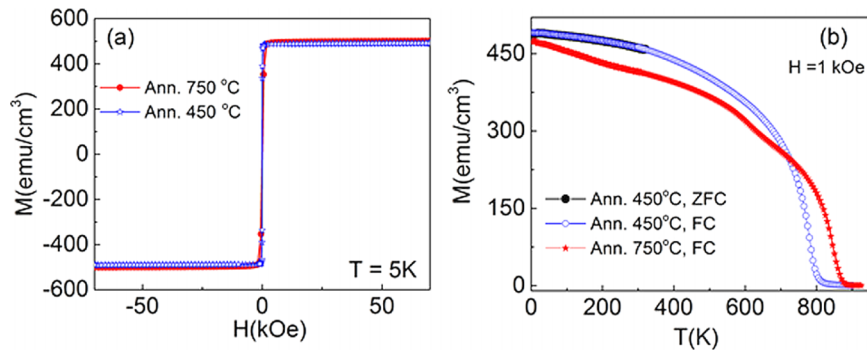


FIG. 2. Structure and magnetism of $\text{CoFeCrAl}_{0.5}\text{Si}_{0.5}$: (a) room-temperature powder XRD patterns of $\text{CoFeCrAl}_{0.5}\text{Si}_{0.5}$ annealed at 450 °C for 4 h, and (b) $M(T)$ curves in a field of 1 kOe. The fit criteria obtained from Rietveld analysis of (a) are $R_{\text{exp}} = 5.7$, $R_p = 6.5$, $R_{\text{wp}} = 8.5$, $R_{\text{Bragg}} = 5.5$.

atomic radii of Si and Al. For CoFeCrAl ,⁴ $a = 5.750 \text{ \AA}$, for the $\text{CoFeCrAl}_{0.5}\text{Si}_{0.5}$ samples annealed at 450 °C and 750 °C, $a = 5.711 \text{ \AA}$ and $a = 5.703 \text{ \AA}$, respectively.

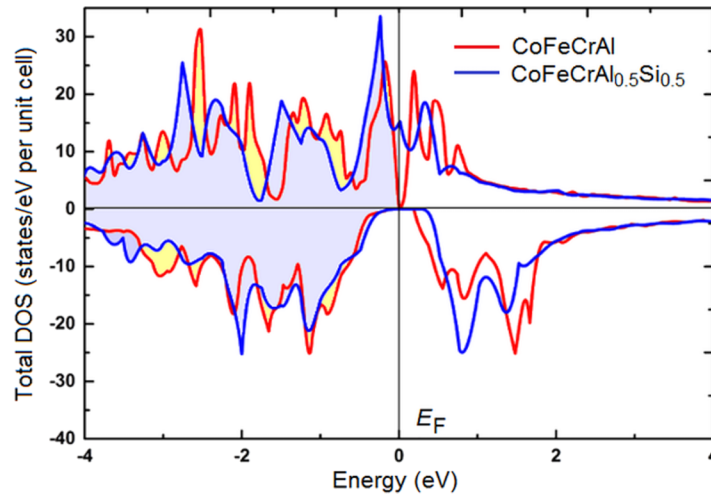
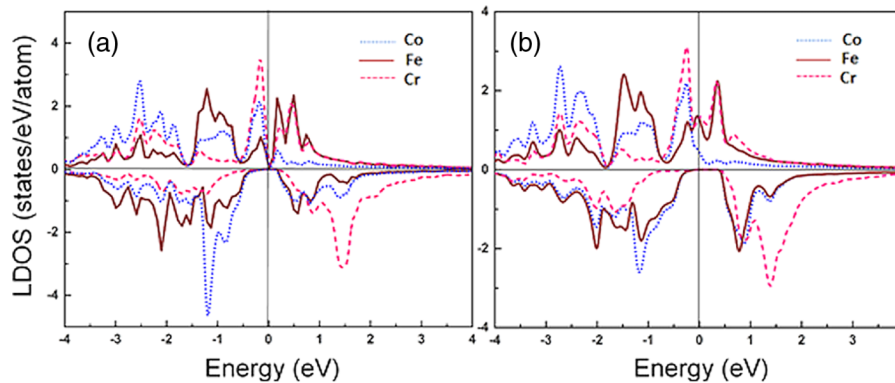
The saturation magnetization at 5 K, about 500 emu/cm^3 ($2.5 \mu_B$ per formula unit) changes very little as a function of the heat-treatment temperature. This value agrees well with the prediction of Slater-Pauling rule for the corresponding half-metallic phases and also with our first-principle calculation (see below). Figure 2(b) shows that the substitution substantially improves the Curie temperature, from 540 K for CoFeCrAl annealed at 600 °C⁴ to 782 K (450 °C annealing) and 845 K (750 °C annealing) in $\text{CoFeCrAl}_{0.5}\text{Si}_{0.5}$. Significant Curie-temperature changes due to substitutions of nonmagnetic elements are not surprising, because the interatomic exchange is affected by both magnetic and nonmagnetic atoms. The $M(T)$ curve of the sample annealed at 750 °C exhibits a dip near 610 K, similar to the dip observed in CoFeCrAl annealed at 700 °C.⁴ This behavior may be caused by impurity phases, but more work needs to be done to understand the finite-temperature magnetism of the system. The $\text{CoFeCrAl}_{0.5}\text{Si}_{0.5}$ samples have very low coercivities, about 100 Oe at 5 K, which is consistent with the cubic crystal structure.

B. Computational Results and Discussion

Atomic disorder in SGS CoFeCrAl and the electronic and magnetic properties of CoFeCrAl and $\text{CoFeCrSi}_x\text{Al}_{1-x}$ were investigated using first principle calculations, employing the generalized gradient approximation (GGA)⁹ for exchange and correlations. The calculations are based on the projector augmented wave (PAW)¹⁰ implemented in the Vienna *ab-initio* simulation package (VASP). Experimental lattice parameters were used, namely $a = 5.750 \text{ \AA}$ for CoFeCrAl and $a = 5.711 \text{ \AA}$ for $\text{CoFeCrSi}_{0.5}\text{Al}_{0.5}$. The Brillouin-zone integration is performed using a $17 \times 17 \times 17$ Monkhorst k -point grid. To represent the electronic wave functions, we have used an energy cutoff of 350 eV.

Our calculations confirm the earlier findings¹⁻³ that *ordered* CoFeCrAl is a spin-gapless ferrimagnetic material. The total magnetic moment of ordered CoFeCrAl is $2.018 \mu_B$ per formula unit and the minority band gap is 0.33 eV. The atomic magnetic moments in relaxed CoFeCrAl are $\mu_{\text{Co}} = 0.94 \mu_B$, $\mu_{\text{Fe}} = -0.56 \mu_B$ and $\mu_{\text{Cr}} = 1.66 \mu_B$. In these calculations, all atoms were relaxed in the unit cell, and Hellmann-Feynman forces on relaxed atoms were less than 0.01 eV/\AA . The convergence scale for the self-consistent calculations was fixed to 10^{-7} eV per cell for the total energy.

To investigate *disordered* CoFeCrAl , we start from the perfectly ordered Y structure and interchange the positions of two neighboring atoms per unit cell. The following interchanges have been considered: (I) one Fe atom and one Co atom, (II) one Fe atom and one Cr atom, and (III) one Co atom and one Cr atom. The calculated total moment per relaxed unit cell are $1.71 \mu_B$ (I), $-0.60 \mu_B$ (II), and $1.05 \mu_B$ (III). None of the disordered CoFeCrAl structures is energetically favorable, and the calculated energy differences per defect are 0.00 eV (Fe-Co), 0.60 eV (Fe-Cr), and 0.81 eV (Co-Cr). In more detail, the energy predicted for the Fe-Co defect is 0.24 meV, but this value is probably below the accuracy of the calculations. These changes are consistent with

FIG. 3. Total densities of states for CoFeCrAl (red) and CoFeCrAl_{0.5}Si_{0.5} (blue).FIG. 4. Local densities of states (LDOS) for the *d*-states of Co, Fe and Cr atoms in (a) ordered CoFeCrAl and (b) CoFeCrSi_{0.5}Al_{0.5}.

the behavior of other Heusler-type alloys,^{11,12} the Fe-Cr and Co-Cr defects differing from the Fe-Co defects by having higher formation energies and a more pronounced effect on the magnetism. Thermodynamically, these values implies nearly complete Fe-Co solid-solution disorder but a substantial degree of L2₁ order (Fig. 1).

Figure 3 compares the total densities of states in CoFeCrAl and CoFeCrAl_{0.5}Si_{0.5}. The experimental and theoretical moments of the *Si*-substituted CoFeCrAl_{0.5}Si_{0.5} are both 2.50 μ_B per formula unit, in agreement with the corresponding Slater-Pauling predictions.¹³ The Si positively affects the minority electrons, increasing the half-metallic band gap from 0.30 eV to 0.43 eV, although this is accompanied by some smearing of the gap. The Si does not affect the shape of DOS very much but it changes the behavior of the alloy from SGS to half-metallic. On the other hand, the increased band gap for minority spins and the improved ordering (§ II) are advantages of CoFeCrAl_{0.5}Si_{0.5}.

Figures 4(a) and 4(b) show the local densities of states (LDOS) of CoFeCrAl and CoFeCrSi_{0.5}Al_{0.5}, comparing the *d*-states of Co, Fe and Cr. In CoFeCrAl_{0.5}Si_{0.5}, the main contribution to the density of states at the Fermi level comes from the Fe atoms. Another feature is the Cr minority states are largely unoccupied, whereas the Cr majority states form a large peak just below the Fermi level. The Si addition slightly changes the transition metal moments, from 0.94 μ_B to 1.06 μ_B (Co), from 1.66 μ_B to 1.68 μ_B (Cr), and from $-0.56 \mu_B$ to $-0.17 \mu_B$ (Fe).

Aside from the effect of Si on Heusler-ordered CoFeCrAl, it is interesting to compare the relative energies of the partially disordered (B2) and Heusler-ordered (Y or L2₁) structures with and without Si substitution. Experiment (Sect. II A) indicates that Si substitution improves the degree of

Heusler-type order, and this trend is confirmed by our DFT calculations. B2 disorder means that Cr atoms interchange positions with Al and/or Si atoms, and the corresponding defect energies can be calculated in the 16-atom supercells of Fig. 1. The energy difference between the Y and B2 structures increases from 0.089 eV per defect in CoFeCrAl to 0.164 eV per defect in CoFeCrAl_{0.5}Si_{0.5}, in agreement with the experimental trend.

III. CONCLUSIONS

In summary, theoretical and experimental methods have been used to investigate structural, electronic and magnetic properties of CoFeCrAl and CoFeCrSi_{0.5}Al_{0.5}. Several types of antisite disorder (Fe-Co, Fe-Cr, Co-Cr) have been considered and compared with the predictions for perfectly Y-ordered CoFeCrAl. None of these antisite defects is energetically favorable, but the energy of the Fe-Co defects is very low, which corresponds to a structure that is basically of the L2₁ (cubic Heusler) type with some B2 disorder, as contrasted to the Y structure. The addition of Si reduces the degree of B2 disorder from 35% to 28%. The predicted electronic structure of CoFeCrAl and CoFeCrSi_{0.5}Al_{0.5}, namely half-metallic ferrimagnetism, is supported by our magnetic measurements. A favorable feature of the Si-substituted alloy is the increase of the minority band gap from 0.30 eV to 0.43 eV.

ACKNOWLEDGEMENT

Theoretical work by R.C. and R.S. is supported by Army Research Office under Award W911NF-10-2-0099, and theoretical research by A.K. is supported by Nano Mission, DST, India (SR/NM/NS-1198/2013). Experimental work at Nebraska by Y.J., A.O'C., and D.J.S. and the writing of the paper by R.S. and R.C. were supported by the U.S. Department of Energy, Office of Basic Energy Sciences under Award DE-FG02-04ER46152. Experimental research by P.K., Y.H., and S.G. at SDSU is supported by Academic and Scholarly Excellence Funds, Office of Academic Affairs. Experimental characterization work by S.R.V. and D.J.S. at Nebraska was performed in part in the Nebraska Nanoscale Facility, Nebraska Center for Materials and Nanoscience, which is supported by the National Science Foundation under Award NNCI: 1542182, and the Nebraska Research Initiative. The first-principle calculations were performed at the Holland Computing Center (HCC) at the University of Nebraska.

- ¹ J. Nehra, V. D. Sudheesh, N. Lakshmi, and K. Venugopalan, "Structural, electronic and magnetic properties of quaternary half-metallic Heusler alloy CoFeCrAl," *Phys. Status Solidi RRL* **7**, 289-292 (2013).
- ² G. Y. Gao, Lei Hu, K. L. Yao, Bo Luo, and N. Liu, "Large half-metallic gaps in the quaternary Heusler alloys CoFeCrZ (Z = Al, Si, Ga, Ge): A first-principles study," *J. Alloys Compd.* **551**, 539-543 (2013).
- ³ G. Z. Xu, E. K. Liu, Y. Du, G. J. Li, G. D. Liu, W. H. Wang, and G. H. Wu, "A new spin gapless semiconductors family: Quaternary Heusler compounds," *Europhys. Lett.* **102**, 17007-1-6 (2013).
- ⁴ P. Kharel, W. Zhang, R. Skomski, S. Valloppilly, Y. Huh, R. Fuglsby, S. Gilbert, and D. J. Sellmyer, "Magnetism, electron transport and effect of disorder in CoFeCrAl," *J. Phys. D: Appl. Phys.* **48**, 245002 (2015).
- ⁵ L. Bainsla, A. I. Mallick, A. A. Coelho, A. K. Nigam, B. S. D. Ch. S. Varaprasad, Y. K. Takahashi, Aftab Alam, K. G. Suresh, and K. Hono, "High spin polarization and large spin splitting in equiatomic quaternary CoFeCrAl Heusler alloy," *J. Magn. Mater.* **394**, 82-86 (2015).
- ⁶ S. Ouardi, G. Fecher, C. Felser, and J. Kübler, "Realization of Spin Gapless Semiconductors: The Heusler Compound Mn₂CoAl," *Phys. Rev. Lett.* **110**, 100401 (2013).
- ⁷ H. Luo, H. Liu, X. Yu, Y. Li, W. Zhu, G. Wu, X. Zhu, Ch. Jiang, and H. Xu, "Effect of Fe substitution on the magnetic properties of half-Heusler alloy CoCrAl," *J. Magn. Mater.* **321**, 1321-1324 (2009).
- ⁸ B. A. Alhaj and B. Hamad, "Electronic and magnetic properties of Co_{2-x}Fe_xCrAl alloys: Ab initio calculations," *Phys. Stat. Sol. B* **251**, 184-189 (2014).
- ⁹ J. P. Perdew, K. Burke, and Y. Wang, "Generalized gradient approximation for the exchange-correlation hole of a many-electron system," *Phys. Rev. B* **54**, 16533-16539 (1996).
- ¹⁰ G. Kresse and D. Joubert, "From ultrasoft pseudo potentials to projector augmented-wave method," *Phys. Rev. B* **59**, 1758-1775 (1999).
- ¹¹ Ph. J. Hasnip, Ch. H. Loach, J. H. Smith, M. I. J. Probert, D. Gilks, J. Sizeland, L. Lari, J. Sagar, K. Yoshida, M. Oogane, A. Hirohata, and V. K. Lazarov, "The Effect of Cobalt-Sublattice Disorder on Spin Polarisation in Co₂Fe_xMn_{1-x}Si Heusler Alloys," *Materials* **7**, 1473-1482 (2014).
- ¹² J. Dubowik, I. Gościńska, Y. V. Kudryavtsev, and V. A. Oksenenko, "Structure and magnetism of Co₂CrAl Heusler alloy films," *Mater. Sci-Poland* **25**, 1281-1287 (2007).
- ¹³ K. Özdoğan, E. Şaşıoğlu, and I. Galanakis, "Slater-Pauling behavior in LiMgPdSn-type multifunctional quaternary Heusler materials: Half-metallicity, spin-gapless and magnetic semiconductors," *J. Appl. Phys.* **113**, 193903 (2013).